Nondestructive Determination of Postharvest Quality of Persimmon Fruit

F15N503F
Phuangphet Hemrattrakun

Doctoral Program in Environmental Science and Technology

Graduate School of Science and Technology

Niigata University

Contents

Chapter 1

Overview

1. Persimmon fruit botany and quality

1.1 Persimmon fruit

Japanese persimmon (*Diospyros kaki* Thunb.) is an attractive fruit with yellow to orange to deep red skin color which is belongs to family Ebenaceae. Persimmon may be spherical, acorn or pumpkin shaped, depending on the variety (Figure 1.1). This plant has been introduced to Japan since ancient times, and superior selections have been recognized and propagated for hundreds of years. Horticulturally, persimmons can be classified into two general categories as astringent and non-astringent persimmon (also called 'sweet' persimmon) (Yonemori et al., 2003). For non-astringent cultivars are normally edible at harvest, whereas astringent types can be consumed only after astringency has been removed.

Figure 1.1 Persimmon fruit characteristics

In both categories, there are cultivars in which fruit astringency is influenced by pollination and presence of seed. Accordingly, persimmon fruit can be classified into four groups as 1) the pollination-constant non-astringent (PCNA); 2) the pollination-variant non-astringent (PVNA); 3) pollination variant astringent (PVA); 4) pollination constant astringent (PCA). Pollination constant cultivars retain their original flesh color, while the flesh of pollination variant cultivars becomes darker. Among there four types, the PCNA and PVNA groups lose astringency naturally during fruit growth and become edible at maturity, while PVA and PCA groups retain their astringency until fruit softening.

1.2 Persimmon production and market

Over the last few decades, interest in persimmon fruit has been increasing worldwide, meanwhile the production increased substantially due to the growing consumption of its fruit, especially in Southeast Asian countries (Fahmy and Kohei, 2016). Asia is the leading producer of persimmon fruit. China, South Korea and Japan are account for 95 percent of worldwide production. Japan takes the third position in this ranking with 0.26 million-ton production level. The primary location for persimmon production includes the following prefectures: Wakayama, Fukuoka, Nara and Gifu. However, persimmon fruit is produced for mostly domestic consumption, while a little amount is exported to Southeast Asian countries.

1.3 Postharvest quality of persimmon fruit

Fresh and dried persimmon fruit are important nutritional product, which recognized as a source of readily available carbohydrates and biologically active

compounds, such as tannins, polyphenols, steroids, dietary fiber, organic acids, minerals and carotenoids, which contribute to the high antioxidant potential of these fruit (Santos-Buelga and Scalbert, 2000). The standard value of total sugar concentration in persimmon fruit is about 12.5 g/100g FW (USDA, 2020), which higher than those widely consumed fruit such as apple, orange, peaches and pears. In addition, the collected data also showed that consuming about 100-150 g of fresh persimmon fruit provides the daily recommended intake of vitamin C (Giordani et al., 2011). Other beneficial effects of persimmon are those associated with the phytochemical action on human body and health as persimmon fruit is particularly rich in vitamin C, carotenoids, and polyphenols, all of which usually considered as powerful antioxidants that protect against free radicals and prevent risk of cardiovascular disease, diabetes and cancer (George and Redpath, 2008; Park et al., 2008; Piretti, 1991; Uchida et al., 1990)

As ripening progresses, physico-chemical changes occur. For persimmon, the main color changes occur during maturation. The external skin color of persimmon fruit is the indicator of physiological maturity and usually used as a non-destructive index for harvesting. During maturation, increased carotenoid production and associated chlorophyll reduction causes persimmon skin color to change from green to yellow to orange and then red (Ebert and Gross, 1985). The color changes that occur during the maturation process run in parallel to gradual flesh firmness loss. Changes in firmness is related to the microstructural changes as parenchyma progressive degrades, more deformed cells are observed, which related to the degradation of pectin (Salvador et al., 2007). Other chemical changes also accompany with fruit maturation, including sugar accumulation, which related to the contribution of ripe fruit taste. Total acidity in persimmon is relatively low even in immature fruit, but does not change with ripening.

Likewise, maturation and ripening are related to the decrease of polyphenol content, which may lead to a lower antioxidant potential.

Table 1.1 Nutritional value of persimmon (100 g of fresh weight of edible part)

Nutritional facts	Amount
Vitamin A (IU)	5400
Vitamin C (mg)	52
Malic acid (%)	0.13-0.14
Protein (mg)	610
Dietary fibre (%)	86.7
Condensed tannin (g)	14.93
Calcium (mg)	9
Phosphorus (mg)	27
Potassium (mg)	203
Magnesium (mg)	11
Pectin (%)	0.52-1.07
Total sugar (mg)	14340
Reducing sugar (mg)	13900
Sucrose (mg)	420
Fructose (mg)	7030
Glucose (mg)	6870
Brix (°)	16.2
Carotenoids (mg)	2.8-8.3
Lycopene (mg)	0.75-4.1
ß-cryptoxanthin (mg)	0.194-1.566
Phenolic compound (g.100g^{-1} dry weight)	8.5
Water (%)	82.03
Food energy (calories)	79

Source: Daood *et al*. (1992), Itoo (1971), Winton and Winton (1935), Roy *et al*. (1995), Brossard and Mackinney (1963), Van Buren (1979), Takekawa and Masumoto (2012), Zhou et al., (2011), Celik and Ercisli (2008)

2. Near infrared spectroscopy (NIRS)

NIRS technique become one of the most used and promising detection methods in the food area because its offers rapid, versatile, inexpensive which avoid complex sample preparation by chemical or physical processes, both solid and liquid samples in different conditions can all be tested without complex pretreatment and provides acceptable accuracy in both qualitative and quantitative analysis (Hou et al., 2008; Xing and Zhang, 2010). NIRS was first used in agricultural applications by Norris (1964). After product is irradiated by NIR radiation, the incident radiation may be reflected, absorbed or transmitted. For reflection, gloss and surface roughness are major inducing factor of the diffuse reflection. Likewise, scattering is the resulted from multiple refractions at phase changes inside the materials especially scattering elements, such as cell wall, starch granules, chloroplasts, and mitochondria. Moreover, scattering is also dependent on size, shape, and microstructure of the particles and may also appear due to heterogeneities, i.e. pores, openings, capillaries that are randomly distributed throughout the samples (McGlone et al., 1997; Blanco and Villarroya, 2002).

On the other hand, absorption bands in near infrared region mainly correspond to the overtones and combinations of fundamental vibrations from chemical bonds within molecules. In a simple molecule, where it is made up of two atoms, fundamental vibration is made only with the stretching vibration between two atoms. Whilst, in the case of large molecules, where more than two atoms are observed, vibration appears much more complicated because deformation vibration also occurs (Figure 1.2) (Kawano, 1995; Blanco and Villarroya, 2002; Nicolaï et al., 2007).

5
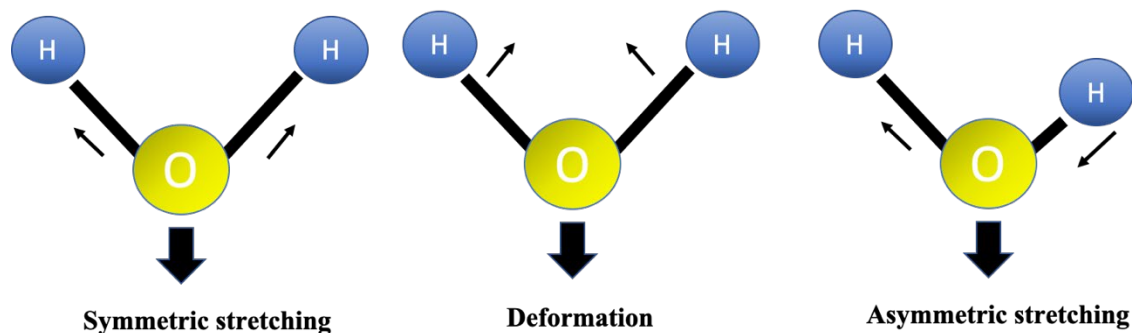
Figure 1.2 Fundamental vibration characteristics of O-H bonds in water molecule (modified from Kawano, 1995)

According to the Beer-Lambert Law, the concentration of an absorber is directly proportional to the sample absorbance as described in following equation.

Equation 1.1 $\qquad$ Absorbance $(A) = \log_{10}(I_0/I_t)$

In which I_0 is the intensity of the incident radiation and I_t is the intensity of the transmitted radiation. This relationship is fundamental to spectroscopy, and it is also frequently applied to the diffuse reflectance of light-scattering materials, replacing I_t with I_r, the intensity of remitted radiation.

2.1 Near infrared radiation

NIR is the section of electromagnetic spectrum that covers the interval between 800 and 2500 nm. The range can be divided into two phases as short-wave NIR (800-1100 nm) and long-wave NIR (1100-2500 nm) ranges as described by Osborne et al. (1993) and illustrated in Figure 1.3.
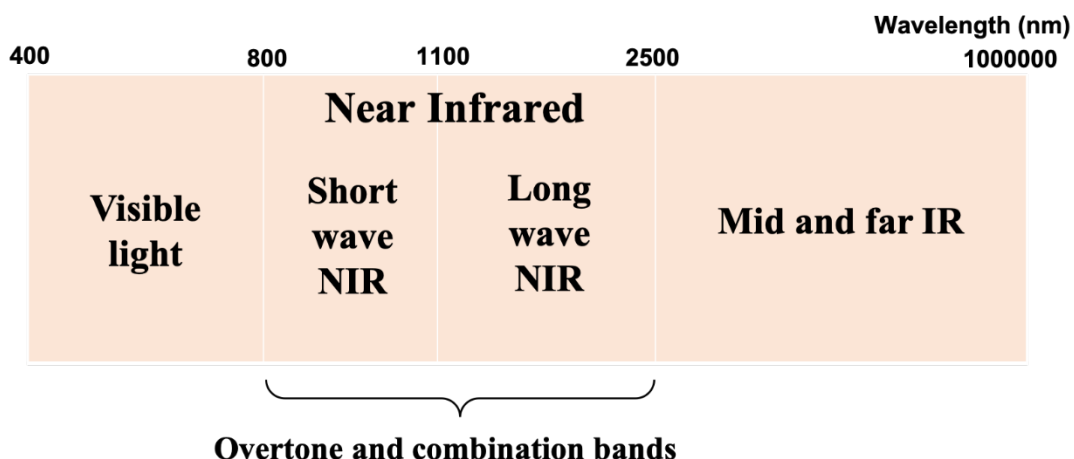
Figure 1.3 The spectral range of visible light and infrared region (modified from Osborne *et al*., 1993; and Kawano, 1995)

The energy of near infrared radiation is coherently related to bond vibration within chemical molecules where the NIR electromagnetic energy is absorbed. Near infrared radiation absorbed by a molecule causes individual bonds to vibrate in a manner similar to that of a diatomic oscillator (Osborne et al., 1993). In large molecules and complex mixtures, such as foods, the multiple bands and the effect of peak-broadening result in NIR spectra that have a broad envelop with few sharp peaks where the multivariate statistical techniques are essential to extract useful information from NIR spectrum (Wold *et al.*, 2001; Nicolaï *et al.*, 2007).

2.2 NIR apparatus and principle

Typical spectrophotometer consists of a light source, which is usually a tungsten halogen light bulb, sample presentation accessory (i.e. irradiating chamber and sample holder), monochromator, detector, and optical components, such as lenses, collimators, beam splitters, integrating spheres and optical fibers. Then, NIR spectra are literally

read out by computational numbers and/or graphic dimensions (Nicolaï et al., 2007). Commercially, NIR instruments are manufactured using one of three geometries to collect reflected light from samples: integrating sphere, large solid angle detector, and small detector. The large solid angle detector offers good collection efficiency, simplicity of construction, and minimum interference from specular reflectance are equipped (Gunasekaran and Irudayaraj, 2001).

2.3 Sample presentation

Typical NIR instruments, rather than absolute absorbance, relative one is usually measured by using a reference material such as ceramic plate or Teflon material. The intensity of light transmitted through a reference material is generally measured. Then the same NIR measurement is performed by using samples in place of the ceramic (or Teflon) plate. Relative absorbance can be obtained by the equation 1.2.

Equation 1.2 $\qquad A_s(\lambda) = \log(I_r(\lambda)/I_s(\lambda))$

Where $A_s(\lambda)$ is the relative absorbance of samples at λ nm, $I_r(\lambda)$ is the light intensity of light transmitted through the reference at λ nm, and $I_s(\lambda)$ is the intensity of light transmitted through the samples at λ nm. Then the aforementioned equation can be derived as equation 1.3.

Equation 1.3 $\qquad A_s(\lambda) = A_s^*(\lambda) - A_r^*(\lambda)$

Where $A_s^*(\lambda)$ is the absolute absorbance of the samples at λ nm, and $A_r^*(\lambda)$ is the absolute absorbance of the reference at λ nm. Therefore, in order to sustain NIR measuring condition, $A_r^*(\lambda)$ should be constant, indicating that the using of identical reference during series of experiment is well controlled (Kawano, 2002).

8

2.4 Sample selection

Before NIRS measurement takes place, it is important to optimize the presentation of the sample. Sample selection is the most important factor in developing a good calibration equation. Calibration procedure involves collecting a number of samples, obtaining both reference and NIR data on each sample and deriving a calibration equation from these data by using chemometrics (McGlone *et al.*, 1997; Kawano, 2002). The samples in calibration set should represent universal population and cover future or unknown samples that will be predicted by calibration model. In the case of agricultural products, the sample set should be sufficiently variable in respect of variety (cultivar, for plant materials), producing area, producing year and maturity (Kawano, 2002). The distribution of the constituent (data distribution; S.D.) being calibrated for over the calibration samples is also important. The range of the variability should be as large as that expected in any future sample, and it is usually better to keep a more uniform spread of values over the whole range (Kawano, 1995; Kawano, 2002; Chen *et al.*, 2006).

2.5 Data collection

At the present, there are four different presentations for NIR spectral measurement, namely, reflectance, transmittance, interactance and transflectance. In the case of reflectance, incident light illuminates the surface of the sample and the diffusely reflected light from the surface, or from the portion near the surface, may be detected. In such this measurement, sample should be opaque, such as powder sample form and small granular form (Slaughter et al., 2003; Nicolaï et al., 2007). In transmittance, the light source is positioned opposite to the detector. The incident light illuminates one

side of the sample and transmitted light is detected from the other side. On the other hand, in Interactance measurement, the light source and detector are positioned in the same side therefore a specular reflection (diffused light) cannot directly enter to the detector. In such this mean, a bifurcated cable or other optical fiber arrangement in which fibers leading to the source and detector are parallel to each other and in contact with the sample. As for transflectance, this technique combines transmittance and reflectance presentations. Incident light is transmitted through the sample and subsequently scattered back from a reflector. Typical reflector is made of ceramic or aluminium material which is compatible with the diffuse reflectance characteristics of the instrument (Kawano, 2002; Nicolaï et al., 2007). Therefore, prior to select the measurement method, it is important to know that the penetration of NIR radiation into fruit tissue decreases exponentially with the depth. Knowing instrument specifications and sample's nature (characteristics) are dramatically crucial. Further, depending on the uniformity of the quality attribute within each horticultural commodity, it might be necessary to repeat the spectral acquisition at several positions on the fruit or vegetable (Figure 1.4) (Schaare and Fraser, 2000; Lammertyn et al., 2000)
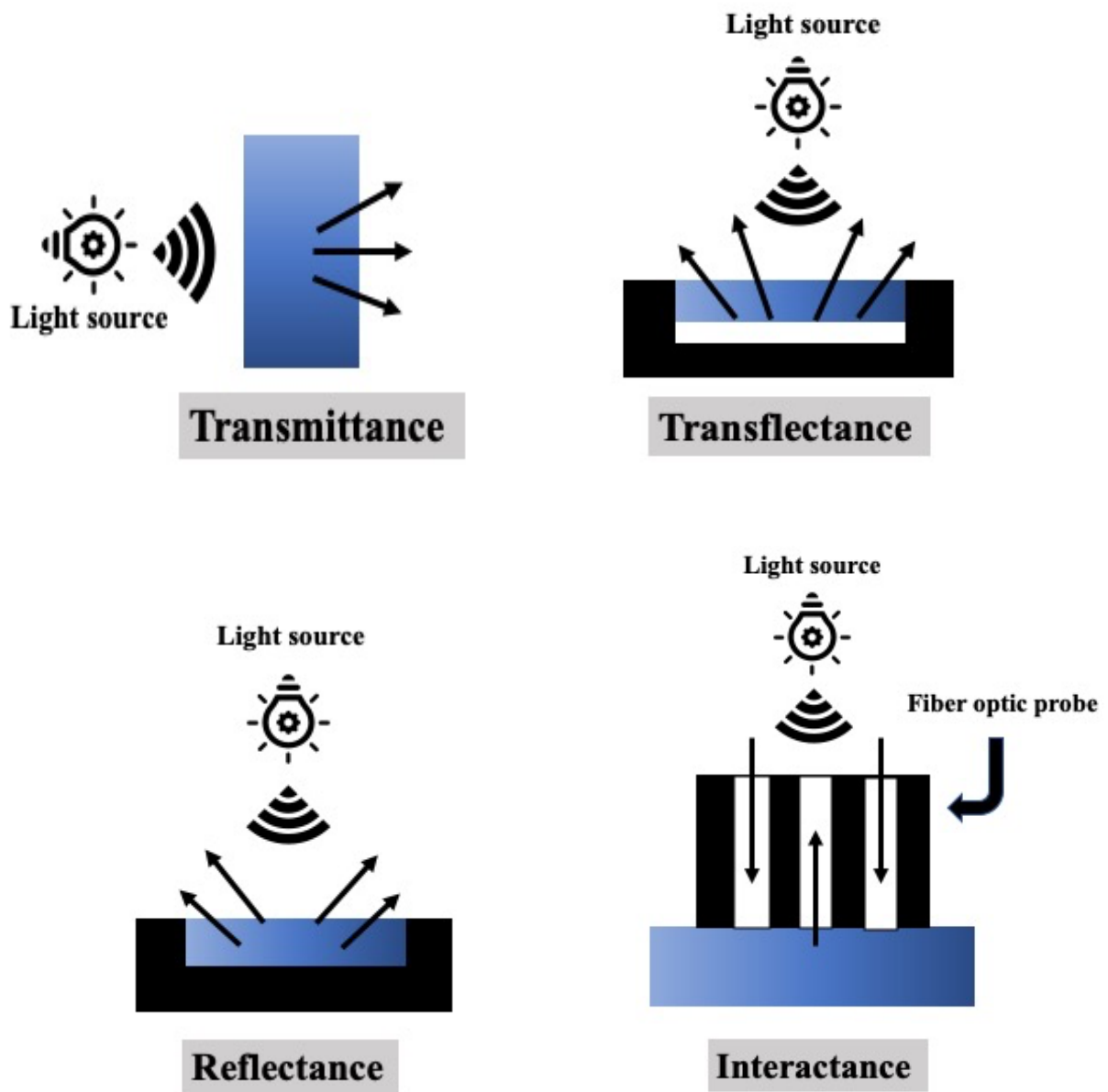
Figure 1.4 Sample presentation and light interactions (modified from Kawano, 1995).

2.6 Pretreatments

There are several well-known pretreatment or pre-processing techniques are used to eliminate unwanted information which cannot be handled properly by the regression techniques. NIR spectra are commonly identified with low-intensity peaks occurring on the shoulders of more intense background spectra. These baselines may occur from scattering in turbid samples, high concentrations of water in the samples, or slight differences in physical properties, for solid samples. All pre-processing techniques have the goal to reducing the un-modeled variability in the data in order to enhance the feature sought in the spectra. By using a suitable pre-treatment, this can be achieved, but there is always the disadvantage of applying the wrong type or applying a too severe pre-processing that will remove the valuable information. The proper choice of pre-processing is difficult to assess prior to model validation, but in general, performing several pre-processing steps is not advisable, and as a minimum requirement, pre-processing should maintain or decrease the effective model complexity (Rinnan et al., 2009).

2.6.1 Derivative

Besides the vast amount of information generated by many types of analytical instrumentation, baseline drift, or drift noise, are also inherently generated. The source and magnitude of these drift effects are highly dependent on the nature of the experiment and the type of instrument used. Instrumental factors such as source intensity fluctuations, detector response variations, temperature fluctuations, spatial correlations in the detection sensors, and physical variations in the sample can all result in drift noise (Brown et al., 2000). Savitzky-Golay (SG) polynomial derivative is among the most frequently used noise-reduction techniques in multivariate calibration from NIR spectra (Savitzky and Golay, 1964). In principle, first-derivative spectra should be free of baseline offset effects, since the first derivative of any function eliminates constant factors (Brown et al., 2000).

Likewise, second- (and higher) derivative spectra reduce baseline effects which can be modeled as polynomial functions of the ordinal variable.

2.6.2 Multiplicative Scatter Correction (MSC)

In order to correct baseline shift and multiplicative effects occurred by physical features such as particle size and sample un-uniformity, MSC is the most famous technique for normalizing NIR spectral data prior to calibration model construction (Næs et al., 2004). Scattering theory is based on the proposition that scattering should have a multiplicative effect on reflectance signal, hence, the observed spectra will contain a broad, changing background from differential scattering at each wavelength. The MSC algorithm was developed to reduce this light scatter effect on diffuse reflectance NIR spectra.

2.6.3 Standard normal variate (SNV)

SNV is a transformation that is usually applied to the spectroscopic data to minimize the effects of light scattering. It uses the centering and scaling of each individual spectrum. The practical result of SNV is that minimizes multiplicative scatter interference in the spectral data produced by the different particle sizes in the sample.

2.6.4 Orthogonal signal correction (OSC)

The OSC for NIR spectral correction was initially introduced by Wold et al. (1998). The core principle of OSC technique is to exclude variations that are not related to the predicted parameter. It does this without eliminating essential information as some other processing method might do (Wold et al., 1998). With OSC, the assumption is that any variation not related to the response variable is an artifact and should be filtered without removing any vital information (Wold et al., 1998; Engel et al., 2013). This is achieved by ensuring that the omitted component is either mathematically orthogonal to the response, or as close to orthogonal as possible.

2.7 Model development

2.7.1 Quantitative analysis

The usual method of calibration of NIR instruments is by multiple linear regression of the reference data on the spectral data. The difficulty in this is two fold. Firstly, NIR spectra contain a large amount of data whereas only a few terms should be included in a regression equation. Secondly, because of the effect of scatter, the raw NIR data are highly intercorrelated and this precludes the use of forward stepwise regression (Osborne, 1983).

2.7.1.1 Multiple linear regression (MLR)

Wavelength is selected based on their correlations with quality parameters. MLR is a multivariate method that employs more than one variable (X) to predict a responded Y value (Osborne et al., 1993). For instance, a stepwise multiple linear regression (SMLR) is a method that also helps to select the variables (X) based on correlation levels, however, SMLR continually selects numbers of variables for calibration input until no further significant of prediction accuracy is obtained. The general MLR (or SMLR) calibration equation can be described according to equation 1.4

Equation 1.4 $Y = a_0 + a_1X_1 + a_2X_2 + a_3X_3 \ldots + a_nX_n$

Where Y is the concentration of constituent of interest, X_1, X_2, $X_3 \ldots X_n$ are absorbance at each wavelength, and a_0, a_1, a_2, $a_3 \ldots a_n$ are regression coefficients calculated by least squares.

2.7.1.2 Principle component regression (PCR)

A useful multivariate regression combines a principle component analysis to MLR fitting by using a representative principle components (PCs) instead of original variables (Nicolaï et al., 2007). The PCR equation can be described according to equation 1.5

Equation 1.5 $Y = a_0 + a_1PC_1 + a_2PC_2 + a_3PC_3 \dots + a_nPC_n$

Where Y is the concentration of constituent of interest, PC_1, PC_2, PC_3, … PC_n are the PCR scores at each PC and a_0, a_1, a_2, a_3 … a_n are regression coefficients calculated by least squares.

2.7.1.3 Partial least square regression (PLSR)

Statistically, the PLSR technique helps to simplify the relationship between X-data (NIR spectral data) and Y-data (chemical and physical data) by ensuring all latent variables are ordered according to their relevance for predicting Y. The method reduces a large number of original spectral data into a much smaller number of factors (F) (Wold et al., 2001). Furthermore, in PLS modeling, the variable importance in projection (VIP) scores are created. The score is a sum of squares of the PLSR-weight, and is a statistic that summarizes the contribution a variable makes to the model. The PLS equation can be described according to equation 1.6.

Equation 1.6 $Y = a_0 + a_1F_1 + a_2F_2 + a_3F_3 \dots + a_nF_n$

Where Y is the concentration of constituent of interest, F1, F2, F3 … Fn are the PLS scores at each factor (F), and a0, a1, a2, a3 … an are regression coefficients calculated by least squares.

2.7.2 Qualitative analysis

Qualitative or discriminant analysis is a way to build classifiers: that is, the algorithm uses labelled training data to build a predictive model of group membership which can then be applied to new cases. While regression techniques produce a real value as output, discriminant analysis produces class labels. As with regression, discriminant analysis can be linear, attempting to find a straight line that separates the data into categories, or it can fit any of a variety of curves. It can be two dimensional or multidimensional. In higher dimensions the separating line becomes a plane, or more generally a hyperplane. Discriminant analysis also outputs an equation that can be used to classify new examples (Hallinan, 2012).

2.7.2.1 Linear discriminant analysis (LDA)

LDA is a simple classification method, mathematically robust, and often produces robust models, whose accuracy it as good as more complex methods. LDA assumes that the various classes collecting similar objects (from a given area) are described by multivariate normal distributions having the same covariance but different location of centroids within the variable domain (Leardi, 2003)

2.7.2.2 Quadratic discriminant analysis (QDA)

QDA is a probability-based parametric classification technique that can be considered as an evolution of LDA for nonlinear class separations. QDA also assumes that

probability density distributions are multivariate normal but it admits different dispersions for the different classes. Consequently, the probability distribution of each class is described by its own variance-covariance matrix and the ellipses of different classes differ for eccentricity and axis orientation (Geisser, 1964)

2.7.2.3 Partial least-squares discriminant analysis (PLS-DA)

PLS-DA is a supervised method based on searching an optimal set of latent variable data for classification purposes. It is developed from algorithms for partial least-squares (PLS) regression, employing a set of predictor variables x and a dependent variable y. In PLS-DA, the dependent variable is the so-called class variable, which is a dummy variable that shows whether a given sample belongs to a given class. It has the advantage of being suitable when the number of objects is lower than the number of variables (Martelo-Vidal and Vázquez, 2016).

2.8 Model statistics and validation

2.8.1 Quantitative analysis

Several parameters are used to judge the calibration performance. Many chemometric software packages offer automatic calibration development with implemented criteria to judge the quality of the developed calibration model. Nevertheless, manual observation of the figures of merit is often needed due to the particular variety and complexity of the analytical tasks. Moreover, during calibration it is essential to determine the optimal number of PLS factors to retain in the calibration model. Using too few factors can leave important NIR structures unmodeled, while using too many factors draws too much measurement noise.

17

The statistical parameters including root mean square error of calibration (RMSEC), root mean square error of prediction (RMSEP), ratio of performance to deviation (RPD), coefficients of determination (R2) and prediction (Q2) were used to evaluated the predictive performance of the PLS models (Wongsaipun et al., 2018) These statistical parameter can be calculated as follows:

Equation 1.7 $\qquad$ RMSEC, RMSEP $\quad = \quad \sqrt{\dfrac{\sum_{i=1}^{N}(c_i - \hat{c}_i)^2}{N}}$

Equation 1.8 $\qquad$ R2 , Q2 $\; = \; 1 - \dfrac{\sum_{i=1}^{N}(c_i - \hat{c}_i)^2}{\sum_{i=1}^{N}(c_i - c)^2}$

Equation 1.9 $\qquad$ RPD $\; = \; \dfrac{SD}{RMSEP} \quad = \quad \dfrac{\sqrt{\dfrac{1}{N-1}\sum_{i=1}^{N}(c_i - c)^2}}{\sqrt{\dfrac{1}{N-1}\sum_{i=1}^{N}(c_i - \hat{c}_i)^2}}$

Where, N is the number of samples. RMSEC is the average difference between predicted ($\hat{c}_i$) and expected (c_i) response values in auto prediction mode. On the other hand, RMSEP calculates the error of the predicted response values ($\hat{c}_i$) based on cross validation. The ratio of prediction to deviation (RPD) was used to standardize the predictive accuracy and was calculated as the ratio of the standard deviation (SD) of the reference values and the root mean square error of cross-validation (Wang et al., 2017).

2.8.2 Qualitative analysis

An important issue is to determine how well the model performs. The conventional approach is to divide the data into training and test sets and see how well training set model predict the test set samples. In this case, 2/3 of the fruit samples from each class

membership were randomly selected and used as training samples, while the rest of the samples were used as test samples. This algorithm was repeated 100 times. Several statistics indices based on a majority vote, including percentage predictive ability (%PA), percentage model stability (%MS) and percentage correctly classified (%CC) were computed to evaluate model performance of the classification models (Brereton, 2009; Krongchai et al., 2016).

The PA is a percentage of times that a sample is correctly classified. For example, using 100 iterations, if a sample is picked up 60 times to be used as a test sample and from these 60 iterations if there are 45 times that this sample is correctly classified, then it means that the PA for this sample is 75%. The MS is an index to indicate the stability of a model when it is used to predict a sample. When PA is available can be related as follows:

Equation 2.0 $\%MS = 2(|\%PA - 50|)$

Lastly, the CC index measures how often a sample is correctly classified and determines the voting result. If a sample is classified more frequently (in this work, %PA > 50%), it is then determined to be correctly classified. For example, if there are 40 samples, and 30 have PA greater than 50%, the CC is 75%.

3. Robustness of NIRS

Calibration equation is called as robust when the prediction accuracy is relatively insensitive towards unknown changes of external factors. The main factors which may affect equation performance are listed as follows:

- The calibration equation developed on one instrument and transferred to another instrument that produces instrumental responses that differ from the responses obtained on the first instrument.
- The instrument responses measured on a single instrument drift because of temperature fluctuations, electronic drift, and changes in wavelength of detector stability over time.
- The sample belongs to different batches.

Therefore, aiming to obtain a robust calibration equation, it is important to develop the model based on sufficient samples; meaning cover broad range of samples, orchards, seasons and years (Kays et al., 2000; McGlone et al., 2002; Nicolaï et al., 2007; Teerachaichayut et al., 2007).

4. NIRS application

Due to its precise and fast analytical characteristics, NIRS is being one of the presently most widespread modern analytical techniques. Likewise, there are numbers of publications present the importance of NIR technique in postharvest technology, as well as many manufactures have implemented NIR systems in grading lines for measure various quality attributes of product such as soluble solids content, starch content and dry matter (Blanco and Villarroya, 2002; Nicolaï et al., 2007). Previous researches have demonstrated the potential of NIR technology for quantitative characterization of fruits. Xie et al. (2011) analyzed organic acid in bayberry, while Pedro and Ferreira (2007) applied the same methodology (NIR) to predict sugar content and acidity in tomato products. Likewise, Maniwara et al. (2014) used visible and short-wave near infrared spectroscopy for evaluating passion fruit quality. Furthermore, as the propagation of NIR radiation in fruit

and vegetable tissue is affected by their microstructure. NIRS can be used to measure microstructure-related attributes, such as stiffness (Lammertyn et al., 1998), internal damage (Clark et al., 2003a), and even sensory attributes (Mehinagic et al., 2004). Likewise, Terdwongworakul et al. (2012) determined the translucent content in mangosteen by means of near infrared transmittance. As translucent flesh disorder is undesirable in mangosteen meant for export. Moreover, Mowat and Poole (1997) successfully classified persimmon into the varieties Fuyu and Matsumoto Wase Fuyu based on different maturity characteristics using visible-NIR reflectance mode.

5. Objective

Currently, consumption of fruit and vegetables is gaining considerable importance as safeguard to maintain human health. Likewise, functional materials, such as ascorbic acid (vitamin C) and polyphenols, are present in persimmon fruit. Although several studies of non-invasive techniques are used and implemented in various types of agricultural products, however, some report have shown unsatisfactory results on persimmon fruit. This study consequently aims at (i) to determine the ability of NIRS in predicting physical and chemical quality of persimmon fruit and (ii) to compare the measurement techniques among interactance and reflectance.

Chapter 2

Comparison of reflectance and interactance modes of visible and near infrared spectroscopy for predicting persimmon fruit quality

Abstract

The principal aim of this work was to compare the ability of measurements technique among interactance and reflectance in predicting soluble solids content (SSC), ascorbic acid (ASC) and firmness of intact persimmon fruit by using visible/short-wave near infrared (Vis/SWNIR) spectroscopy. Calibration models were developed by partial least square (PLS) regression that related near infrared (NIR) spectra to reference values. The root mean square errors of calibration (RMSEC), the root mean square errors of prediction (RMSEP), the correlation coefficients of calibration (Rcal) and prediction (Rval) and the ratio of performance to deviation (RPD) were used to consider the model accuracy. The PLS models from interactance showed satisfactory performance, providing better prediction results than reflectance technique in all parameters. ASC and firmness presented the best calibration models. ASC, Rval = 0.92, RMSEP = 5.56 (mg kg-1 FW) and RPD = 2.54 were attained when using orthogonal signal correction (OSC) pretreatment. Firmness, Rval = 0.89, RMSEP = 4.21 N and RPD = 2.14 were also achieved using OSC pretreatment. These findings highlighted the potential of Vis/SWNIR spectroscopy with the multivariate calibration technique to be applied for evaluating ASC and firmness of fresh persimmon fruit.

1. Introduction

Persimmon (Diospyros kaki Thunb.) is a widely cultivated crop worldwide (Yonemori and Sugiura 2000). Over the last few decades, the production of persimmon fruit has grown substantially because of the growing consumption of its fruit in Southeast Asian countries (Fahmy and Kohei 2016). Persimmon fruit can be categorized by the astringent taste at harvest time, also with their response to pollination and presence of seed. These cultivars are divided into four types as pollination constant astringent (PCA), pollination constant non-astringent (PCNA), pollination variant astringent (PVA), and pollination variant non-astringent (PVNA) (Yonemori and Sugiura 2000). Additionally, it is an edible fruit that contains primarily natural vitamin C sources (USDA 2016). The collected data suggests that consuming about 100–150 g of fresh persimmon fruit provides the daily recommended intake of vitamin C (Giordani et al. 2011). Furthermore, the fruit is also abundant with carbohydrates, mainly fructose, glucose and sucrose (Candir et al. 2009; Del Bubba et al. 2009; Veberic et al. 2010). However, among the Diospyros species, Diospyros kaki is the most important from a nutritional point of view (Zheng et al. 2006). Barrett et al. (2010) claimed that characteristics that impart distinctive quality consisted of four different attributes, including (1) colour and appearance, (2) flavour, (3) texture and (4) nutritional value. The appearance is one of the critical parameters for determining the acceptability of each product by visual inspection. Meanwhile, other attributes, as aforementioned, are hidden characteristics that have become increasingly valued by consumers in nowadays, especially for the nutritional profile that appears to provide additional benefits for people with different health concerns. Therefore, since the demand for good-quality product is increasing, using efficient and effective ways for quality assessment is desirable for postharvest handling system.

23

Several spectral analysis techniques are widely implemented to evaluate the quality attributes of watermelon (Jie et al. 2013), passion fruit (Oliveira et al. 2014; Maniwara et al. 2014; Maniwara et al. 2019) and tangerine fruit (Theanjumpol et al. 2019). However, near-infrared (NIR) spectroscopy represents one of the most broadly used techniques in food chemistry, which is recognized as a rapid, non-destructive, low-cost and robust analytical method (Nicolaï et al. 2007a; Lopez et al. 2013; Vitale et al. 2013). Cortés et al. (2017) examined the feasibility of Vis/NIRS for determining the astringency of intact and the flesh of persimmons. Their results showed that using partial least square regression (PLSR) gave a high correlation (R = 0.904), demonstrating the potential of this technique for astringency assessment of persimmon fruit. Wang et al. (2017) generated the regression model for predicting SSC and firmness of European pears using portable Vis/NIR spectroscopy, and the results presented a more reliable of prediction, which was obtained by using the OSC pre-processing technique coupled with PLS regression model (R2 = 0.87). Nordey et al. (2017) assessed mango internal quality using PLSR along with variable selection and pre-processing of NIRS spectral data. Results revealed the importance of pre and postharvest factors that could lead to NIRS models development and robustness in prediction. Maniwara et al. (2014) conducted postharvest quality investigation for passion fruit by using Vis/SWNIR. The best PLS model for predicting SSC was obtained from interactance measurement mode, and the developed model showed 0.923 of a correlation coefficient between measured and predicted values.

The objective of this research were (i) to determine the ability of NIRS in predicting persimmon fruit quality and (ii) to compare the measurement techniques among interactance and reflectance.

2. Material and methods

2.1 Sample preparation

For this study, 124 Persimmons (Diospyros kaki Thunb.) cv. Hiratanenashi, PVA type cultivar, were purchased immediately after harvest from Niigata prefecture, Japan. The collection time was corresponding to late September and mid-October of 2016. Removal of astringency from persimmon fruit was achieved by exposing 'Hiratanenashi' persimmon fruit to 90–100% carbon dioxide (CO_2) for 24 h at 20±2 °C. This treatment induced the anaerobic respiration, resulting in the accumulation of acetaldehyde, which precipitates the soluble tannin during the fumigation treatment. Thus, the astringency taste is eliminated (Matsuo et al. 1991). The sorted persimmon fruit was stored at ambient air temperature overnight (20±2 °C, RH 60–80%) before Vis-SWNIR spectral measurements were conducted on the next day. Morphological properties of persimmon samples, including diameter, height and weight were recorded prior to each spectroscopic measurement. The uniform of fruit size and shape being carried out from the height to diameter ratio as a fruit shape index. The diameter and height of persimmon fruit were calculated by digital calliper (SK-calliper, SK Niigata Seiki Co., Ltd., Niigata, Japan). The weight was measured by electronic balance (AND GX-600, A & D Co., Ltd., Tokyo, Japan).

2.2 Visible and Near-Infrared Spectra Acquisition

All Vis-SWNIR spectra (310–1100 nm with a 3.3 nm interval wavelength) were recorded as the logarithm of reciprocal absorbance (log1/R) by using a spectrophotometer (Handy Lambda II, Spectra Co., Ltd., Tokyo, Japan). The spectra were firstly collected in reflectance mode; the lamp used was 12-V/100-W tungsten halogen lamps (MCR 12-150 M). Thereafter, interactance spectra of each fruit were made by a portable fibre optic probe

module containing the light source (MHAA-100W, Moritex Co., Ltd., Saitama, Japan). The orientation angle between light source and fibre optic detector probe was set at a 45° angle and in direct contact with the fruit surface (0° angle) for the reflectance (Fig. 4b) and interactance (Fig. 4a) measurement procedure, respectively. Each fruit was scanned perpendicularly at four sites along the equatorial positions. Each spectrum was accumulated from ten continuous acquisitions in the marked region. Thus, a total of 40 scans were automatically averaged for each fruit. The reference spectrum was conducted by using a white ceramic plate (1.5 mm thickness) every time after examining five fruit to recalibrate the NIR apparatus. The spectra were acquired and transformed by the Wave Viewer software (Spectra Co., Ltd., Tokyo, Japan) and the Unscrambler®X version 10.4 (CAMO software, Oslo, Norway), respectively. Fig.1 shows the average spectra (absorbance) of persimmon fruit from interactance (Fig. 1a) and reflectance (Fig. 1b) measurements.
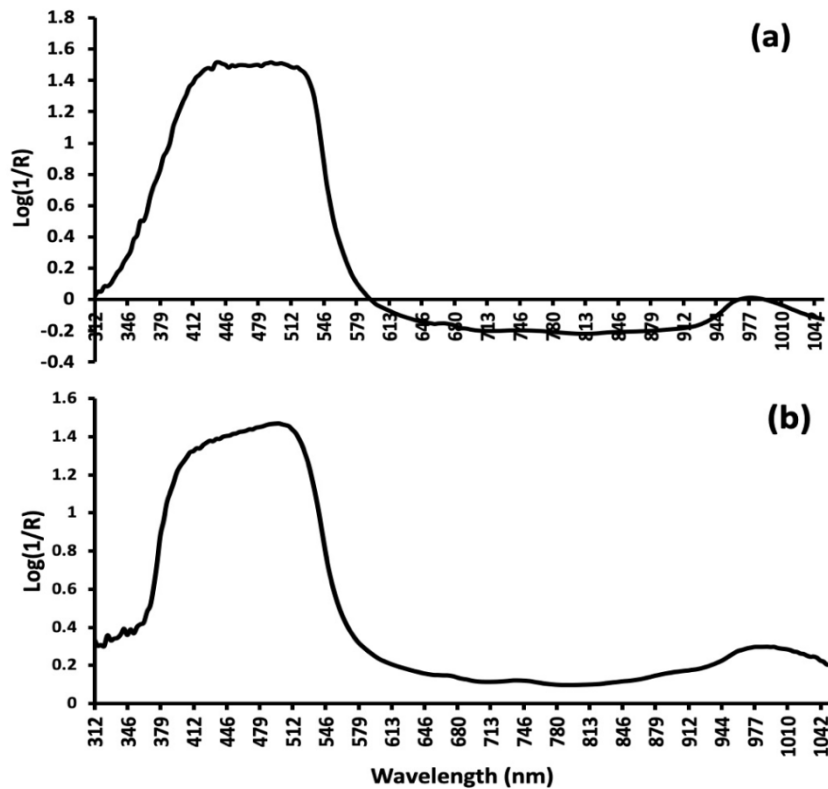

Fig 1. Typical average NIR spectra of intact persimmon fruit for interactance (a) and reflectance (b)

2.3 Determination of fruit quality parameter

After non-destructive measurements using spectroscopy technique had been completed, SSC, ASC and firmness of the tested persimmon fruit were measured by conventional destructive methods from the same location where Vis-SWNIR spectroscopy had been carried out. Firmness values derived from a standard flat-plate compression (diameter 2 mm) using a Digital Force Gauge (model: FGJN-50, Shimpo Co. Ltd., Tokyo, Japan). Flesh firmness measurement was carried out in kilograms and converted to Newtons by multiplying by 9.81.

For chemical analysis, a circular wedge (20 mm diameter) from the measurement position of each fruit was manually squeezed through a cheese cloth (0.25 mm2 porosity) for filtration, then its SSC determination was performed using a digital refractometer (PR-101α, Brix 0.00-45%, Palette Series, Atago Co., Ltd., Tokyo, Japan). Analysis of ASC content was processed by mixing 1 mL of extracted fruit juice with 2% metaphosphoric acid solution, then dip appropriate test strip into the mixture and subsequently measured for its ASC by using a digital reflectometer (RQflex 10, Merck & Co., Inc., Darmstadt, Germany) (Mijowska et al. 2016). Lastly, NIRS calibration models were developed separately based on these reference parameters. The mean and standard deviation values were determined for each quality parameter.

2.4 Chemometric procedure

To generate a calibration model with high robustness, 97 intact persimmon fruits were used as a calibration set. For the remaining, 27 fruit were used for an external test set. Additionally, to avoid the selection bias, all samples for calibration and validation set were conducted by random sampling in the ratio 3:1. As it is widely known, NIR spectra may comprise undesired information, such as scatter and baseline shift. It is a usual practice to

apply an appropriate spectral pretreatment in suppressing and facilitating all variations of calibration model (Palou et al. 2014). Hence, five spectral pre-processing methods and their combinations were applied with the purpose of achieving reliable and accurate calibration models. These methods included Savitzky-Golay first (1-Der) and second (2-Der) derivatives, multiplicative scatter correction (MSC), extended multiplicative scatter correction (EMSC), orthogonal signal correction (OSC) and standard normal variate (SNV). All spectral pretreatment and regression models were carried out using The Unscrambler®X version 10.4 (CAMO software, Oslo, Norway).

Thereafter, predictive models were developed for the linear relationship between spectral data and reference value using PLS regression. Each model was tested internally via full-cross validation to determine complexity using the number of factors that presented the root-mean-square error in cross validation (RMSECV). Once optimised on the calibration set, the prediction test was applied to spectra of external validation samples to test their feasibility. Afterwards, the predictability of each constituent was explained by Rcal, Rval, number of factor and RMSEP. The effective and reliable model were defined by Rcal as 0.71 or higher, as described by Williams (2007). In addition, the predictive deviation or RPD was calculated using the ratio of standard deviation (S.D.) to the RMSECV or the RMSEP. Meanwhile, higher values for RPD implied the increasing reliability and precision of the models. Ideally, in an excellent model, the RPD should be greater than 2. Moreover, the important variable (wavelengths) in PLS model analysed for each parameter is presented by loading.

3. Results and discussion

3.1 Physical and chemical quality of persimmon fruit

The quality pattern of the samples showed the uniform distribution of size and shape based on the standard size available in domestic and export market, with a mean of fruit index of 0.68 (Table 1S, supplemental material). The values, mean and standard deviation for the three determined parameters (SSC, ASC and firmness) of the persimmon fruit samples were shown in Table 1.

Table 1 Summary statistics of persimmon fruit in calibration and prediction sets

Parameter		n	Min	Max	Mean	S.D.	S.E.
SSC (%)	Calibration set	97	13.90	19.00	15.90	1.04	0.11
	Prediction set	27	14.50	18.30	16.00	0.99	0.19
ASC (mg kg^{-1} FW)	Calibration set	97	73.33	154.00	97.33	14.53	1.48
	Prediction set	30	76.00	132.67	99.90	13.46	2.46
Firmness (N)	Calibration set	97	19.70	58.26	41.65	8.01	0.81
	Prediction set	30	21.85	58.26	41.70	8.97	1.64

n = number of samples; Min = minimum; Max = maximum; S.D. = standard deviation; S.E. = standard error; SSC: soluble solids content; ASC: ascorbic acid.

3.2 PLS models for predicting SSC

The characteristics and statistics of the models, with each spectral pretreatment and different pre-processing combinations, are shown in the Table 2S and 3S (supplemental material). The best results were obtained using EMSC + OSC and OSC + 2-Der models for interactance and reflectance measurement techniques, respectively. The prediction model showed the lowest RMSEP = 0.58% and the highest Rval = 0.82 using 6 factors, with the EMSC and OSC processing method (interactance). However, only a 1.73 RPD value was achieved from this model, which was defined by Chang et al. (2001) as part of the fair model category (RPD ranges from 1.4 to 2). Meanwhile, the OSC + 2-Der model

(reflectance) provided the highest correlation coefficient (0.81) with the minimum SEP (0.58), which was obtained using four factors. The optimal number of factors for the PLS model, for SSC (Fig. 2a and 2b), was determined by the lowest RMSECV, which substantially demonstrated the predictive abilities of the smallest RMSEP.

Dominant absorption peak of the SSC parameter was observed around the bands 450–570 nm (Fig. 3a and 3b), which are indicated by blue and green absorbing pigments, give the fruit its external characteristics of yellow-orange and orange-red tones, and this could be related to a major carotenoids present in flesh and peel tissue of persimmon fruit (Ebert and Gross 1985; Yuan et al. 2006). Another dominant peak in this visible region was centred around the bands at 660–673 nm; this could be due to the presence of chlorophyll. After these peaks, as the spectrum entered close to the infrared region, the absorption band from the interactance mode showed another significant correlation loading at 980 nm, since the water content of fruit comprised about 80–90% water (Beever and Hopkirk 1990).

Regarding analysis of the targeted regression models, applying OSC obviously reduced the number of PLS components and provided substantial improvement compared to when there was no pre-processing. Wang et al. (2017), when studying a hybrid method for predicting SSC and firmness of European pear, obtained results showing that OSC-PLS models improved the predictability of the model, especially for the SSC parameter. Moreover, the performance of the OSC-PLS also presented higher RPD and greater coefficients of determination. Interesting results were also obtained for predicting quality parameters of straw wine, the combination between OSC and PLS regression demonstrated the improvement of the performance of regression model by reducing the model complexity and prediction error, and also improve the accuracy of model (Croce et al. 2020).

The validation results in Table 2 showed that the developed prediction model of SSC was not completely successful for both measurement modes. Considering RPD values of PLS regression for estimation of SSC content, the display of an RPD value less than 2 generally indicated the influence of disturbance, which caused less accurate prediction. Above this point, it could be the interference of soluble tannins, which naturally presented in the astringent persimmon variety. Noypitak et al. (2015) observed astringency and tannin content in "Xichu" persimmons using near infrared spectroscopy and found that it was the accumulation of acetaldehyde under CO_2 treatment of this type of fruit leading to the transformation of soluble tannin into insoluble form. Meanwhile, after de-astringent treatment, the flesh near the skin still presented higher content of the soluble tannin in than flesh near the core of fruit, which could be caused by the interferences of light scattering effects, especially with the reflectance mode. From this experiment, the remaining soluble tannin also possibly generated the errors of value determination by reflectometer.

Table 2 Results of model performance by PLS regression with interactance and reflectance measurement mode and different spectral pretreatments

| | | Pretreatment | F | Calibration | | | Prediction | | | | |
				R	RMSE CV	SEC	R	RMS EP	SEP	Bias	RPD
Interactance	SSC (%)	EMSC+OSC	6	0.86	0.71	0.54	0.82	0.58	0.57	-0.13	1.73
	ASC (mg kg^{-1}FW)	OSC	5	0.89	8.39	6.52	0.92	5.56	5.31	0.19	2.54
	Firmness (N)	OSC	4	0.87	4.90	4.00	0.89	4.21	4.20	0.86	2.14
Reflectanc	SSC(%)	OSC+2-Der	4	0.79	0.74	0.64	0.81	0.59	0.58	-0.13	1.70
	ASC (mgkg^{-1}FW)	EMSC+2-Der	11	0.87	9.25	7.06	0.84	7.20	7.32	0.02	1.84

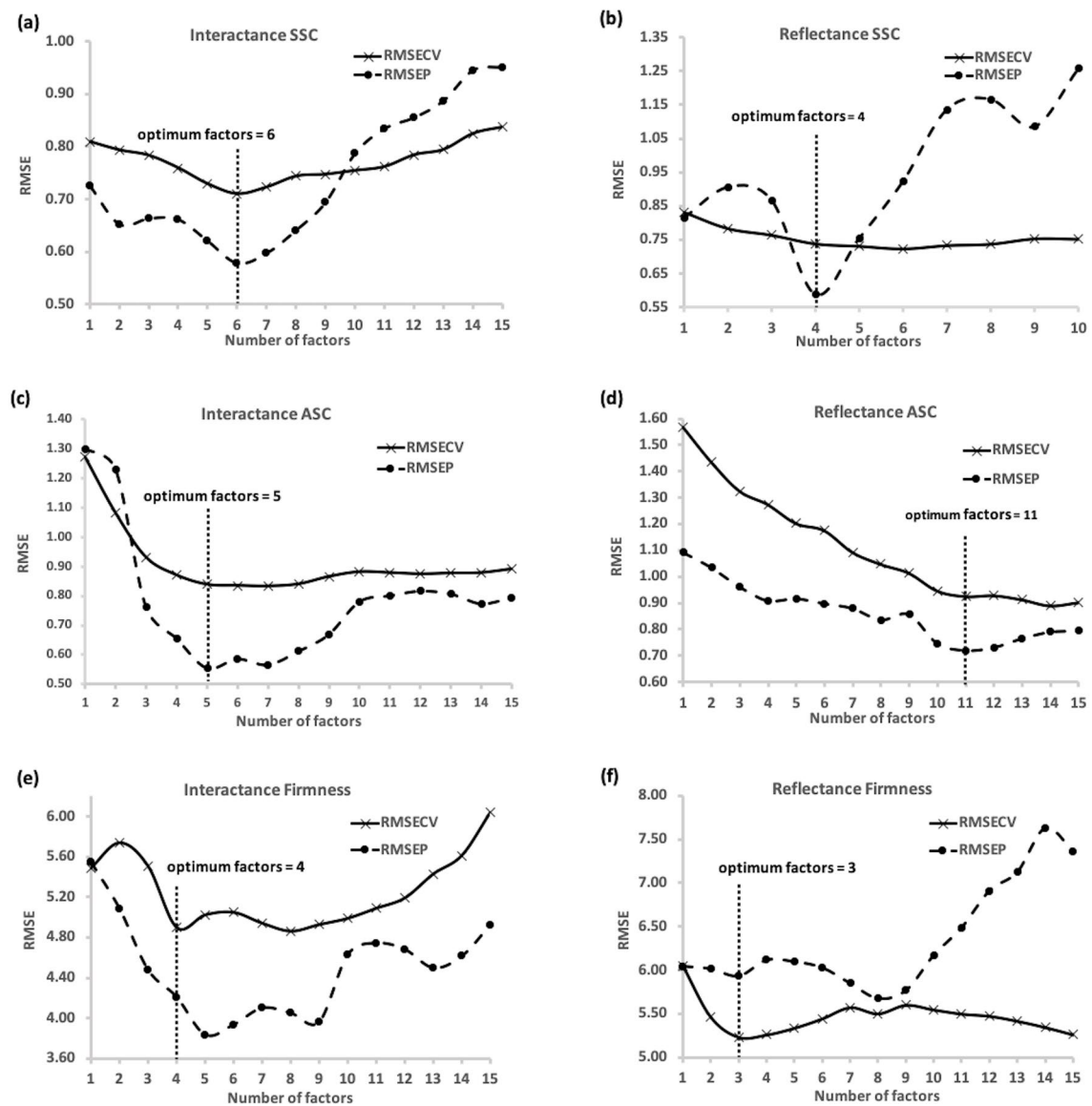| Firmness (N) | EMSC+OSC | 3 | 0.83 | 5.24 | 4.47 | 0.75 | 5.94 | 5.94 | 1.08 | 1.51 |

Fig. 2 Changes of RMSECV and RMSEP, with the number of effective wavelengths included in PLSR analysis of SSC, ASC and firmness modelling. Results from interactance are shown in a, c and e, while b, d and f are derived from reflectance mode measurement

3.3 PLS models for predicting Vitamin C (ascorbic acid)

The calibration models were developed in the range of Vis-SWNIR spectra (310–1100 nm). The calibration and prediction results after applying the spectral pre-processing method is shown the Table 2S and 3S (supplemental material) for interactance and reflectance measurement mode, respectively. For interactance measurement mode, the RMSECV values for ASC ranged between 8.30 and 9.17 (mg kg-1FW), and the RMSEP values were in the range of 5.54–7.45 (mg kg-1FW). Meanwhile, the correlation coefficients of prediction set ranged from 0.83–0.92 for all pretreatments. From Table 2, it can be inferred that OSC decreased the number of factors needed for modelling while providing the highest precision of prediction model with RMSEP = 5.56 and RPD = 2.54, which ensured the accuracy and robustness of the model for the prediction of ASC in persimmon fruit. As mentioned earlier, the OSC acts as a filter by altering the spectrum in order to remove undesirable systematic variations (Yee and George 2003). At the same time, after observing predictive analysis of PLS-ASC by reflectance mode, the model was clearly considered less robust (Rpre = 0.84, RPD = 1.84) than using interactance one (Rpre = 0.92, RPD = 2.54).

The correlation loading plot of the best fitting model established, using interactance and reflectance measurement modes of ASC, are shown in Fig. 3c and 3d, respectively. Considering these two diagrams, high correlation loading refers to a high influence wavelength for prediction. There were four optimum wavelengths (513, 548, 673 and 970 nm) were identified for the prediction by interactance mode (Fig. 3c). Wavelength 513 nm and 548 nm are related to peel and flesh colour of persimmon fruit, since it corresponds to orange-red colour. However, the band 673 nm could be linked with the chlorophyll absorption band. Meanwhile, an absorption peak observed around 980 nm could be assigned to hydroxyl (OH) vibration absorption. At the same time, the chemical structure

of ascorbic acid also contains four hydroxyl groups in its typical structural formula (Liu et al. 2006).

Regarding the regression model for ascorbic acid content estimation of acerola fruit using PLS regression algorithms conducted by Malegori et al. (2017), the study obtained less predictive accuracy despite of good calibration for both analytical devices (Micro-NIR and FT-NIR). Considering these results, there were several factors that might lead to the uncertainty in the prediction results, such as, variation of sample characteristics, calibrating method, and spectral quality. However, it is very interesting to apply variety of pre-processing algorithms in order to handle spectral information appropriately and to approach better predictive modelling. In the present study, the robust efficiency of spectra in diffuse reflectance mode may affected by the light scattering phenomenon during the spectra acquisition (Frizon et al. 2015), which could be influenced by the spherical shape and shiny skin of persimmon fruit. Munera et al. (2017) described the persimmon appearance as wrinkly, with less shine in its skin during the ripening process, clearly affecting the reflectance properties. Additionally, Schaare and Frazer (2000) used difference optical detection techniques to measure the chemical and physical properties (such as SSC, density and flesh colour) of kiwifruit. They claimed that the spectral acquisition by the interactance measurement technique provided the greatest prediction results, preferable to the reflectance spectra. This incident could be related to the less dominant effect of its peel colour on spectra while using interactance measurement mode.
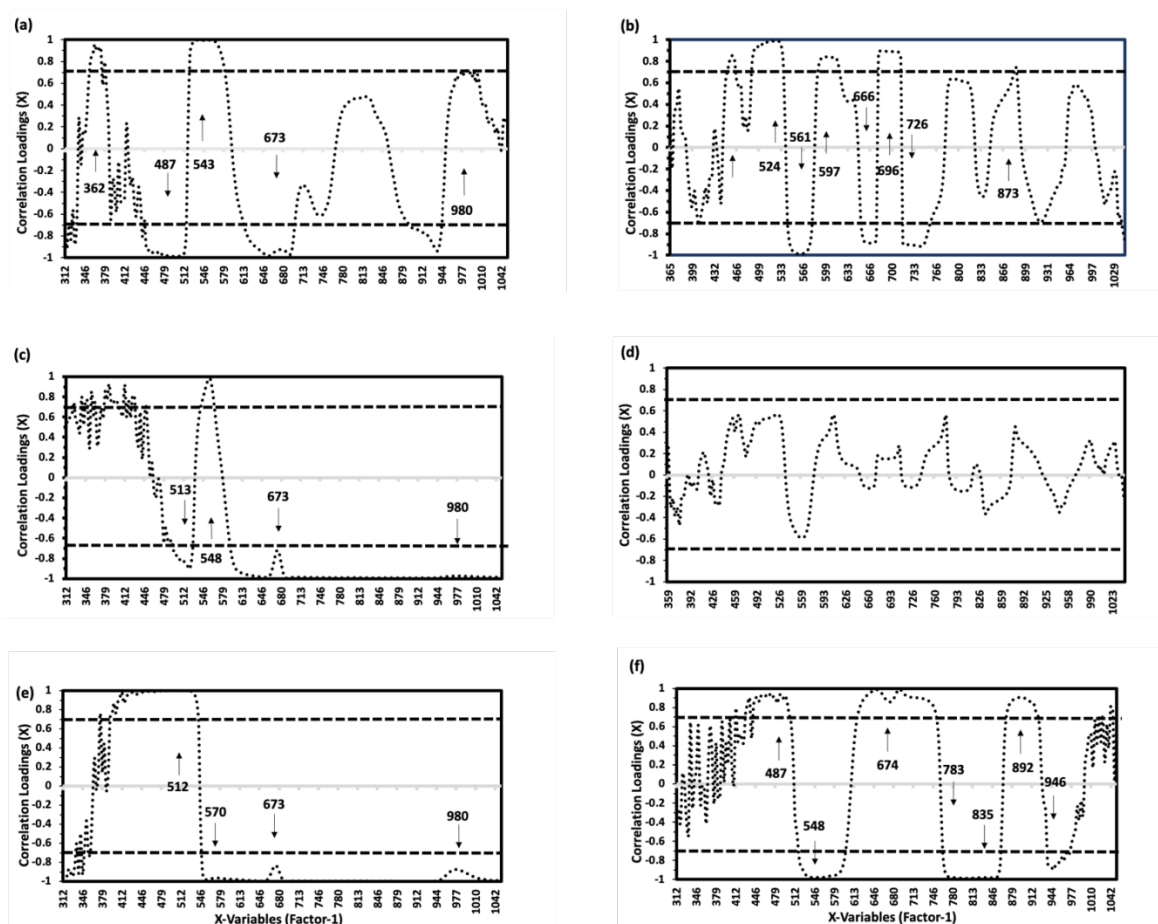
Fig. 3 Correlation Loading of SSC, ASC and firmness modelling using PLSR analysis. Results from interactance are shown in a, c and e, while b, d and f are derived from reflectance mode measurement

3.4 PLS models for predicting firmness

As seen in the Table 2S and 3S (supplemental material), in general, the interactance PLS model for firmness prediction of persimmon fruit showed RMSEP values ranging between 3.97–5.24 N, which was lower than the result from PLS reflectance at 5.80–8.05 N. Meanwhile, in analysing the results obtained from each model of interactance technique (Table 2S, supplemental material), there were only two pre-processing methods which presented an acceptable RPD value (greater than 2.0); these were 2-Der and OSC (RPD =

2.02 and 2.14, respectively). Besides, raw spectrum (without spectra pre-processed) provided the highest RPD value at 2.26, with 10 factors used.

For the firmness prediction results of reflectance measurement mode (Table 3S, supplemental material), the analysis showed poorer predictions than those obtained with interactance. Regarding the RPD values, it was not possible to build a reliable calibration model. For qualitative data analysis as calibration modes, RPD values <1.5 are considered inadequate for most application. The negative result in cases of smaller RPD values can be caused by a narrow range of reference values (small S.D.) or from a large error in prediction results (RMSECV), compared with the reference values variation (Shah et al. 2010; Cozzolino et al. 2011). In this study, the RPD values which were achieved for reflectance were lower than 2.0 for all PLS models. Reflectance measurement also showed notably lower robustness (Rpre = 0.75, RMSEP = 5.94 N) than the prediction performed by interactance (Rpre = 0.89, RMSEP = 4.21 N).

Loadings for prediction model particularly presented dominant absorption bands in the visible region of 400–700 nm. It is well known that the absorption of carotenoid and chlorophyll take place in this region, which is mainly related to peel and flesh colour of persimmon fruit. As maturity increases, the external colour of persimmon fruit changes from yellow-orange to orange-red. However, the ripeness process of persimmon fruit was often accompanied by texture changing, which influenced the firmness parameter. A previous study (Huang et al. 2018) reported high correlation of tomato firmness with the wavelength in the visible region, which was related to chlorophyll and anthocyanin pigment. The absorption peak observed around 800–1,100 nm could be related to the water absorption peak, which may be related to water content increases in the flesh as maturity increases.

However, the application of OSC produced good calibration and prediction results, where the number of factors was reduced considerably compared to the regression model generated from the raw spectra. Palou et al. (2014) discovered the same interference, as the filtered spectral data by OSC did not provide significantly better results of industrial paraffin and oil samples, according to the prediction error (RMSEP), and bias expanded to some extent. Firmness is a physical parameter that indirectly depends on several factors in persimmon fruit. Changes in physiological maturity, as well as the varying of water and sugar content, can cause fruit firmness changes and affect fruit absorption and scattering properties. Therefore, filtering spectral data had varying effects on PLS model predictions. However, an applied pre-processing technique can typically cause the loss of information for prediction, thereby high RMSEP is obtained.

As mentioned above, there are many factors which influence the firmness parameter of persimmon fruit. The firmness parameter mainly measures the structural properties of samples, and an applied pre-processing technique may result in loss of useful information if a proper method is not selected or correctly applied. This might cause lower predictions of the firmness parameter after applying a different pre-processing method.

(a)

Spectrophotometer

Light source

Spectrophotometer

(b)
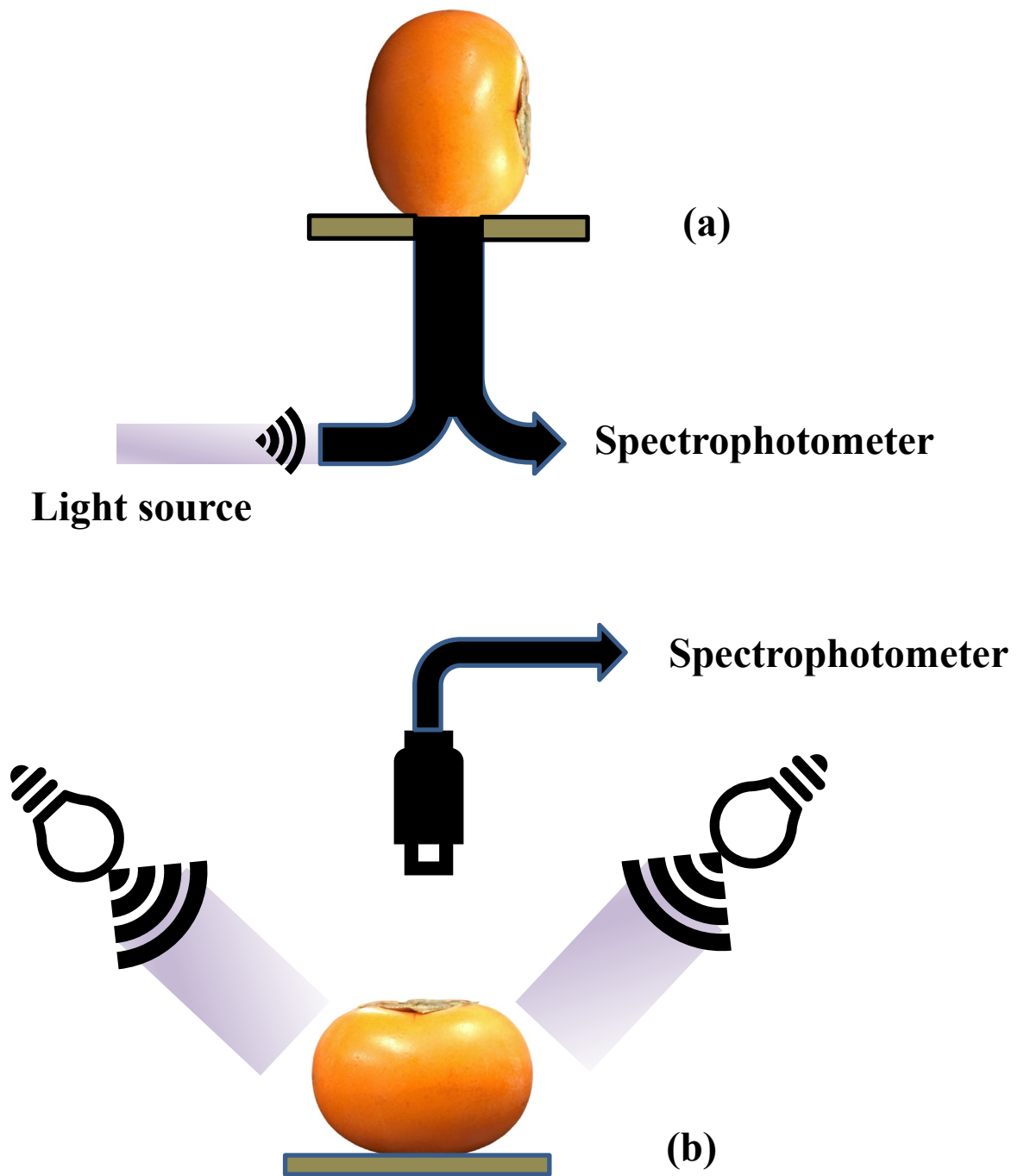
Fig. 4 Schematic representations of interactance (a) and reflectance (b) acquisition modes.

4. Conclusion

In this research, Vis/SWNIRS in interactance and reflectance measurement techniques were studied as potential non-destructive methods to evaluate postharvest quality of persimmon fruit in terms of SSC, ASC and firmness. The results showed that PLS prediction models developed from interactance measurement mode provided the best predictive model for the ASC and firmness, but not the SSC. On the other hand, the PLS model from reflectance technique could not accurately estimated all parameters. This might have been caused by the structural characteristics of fruit, which in turn would affect light scattering. In addition, the use of spectral pre-processing can help minimize unwanted variation. Meanwhile, the other spectral pre-processing and modelling methods should also be considered in order to further improve prediction accuracy. These would be useful for the improvement of postharvest handling of persimmon fruit.

Supplemental material

Table 1S Morphological information of 127 persimmon fruit used in this study. Fruit index: the ratio of height and diameter for the fruit

Parameter	Min	Max	Mean	S.D.	S.E.
Fresh weight (g)	157.34	213.68	198.75	9.58	0.85
Diameter (mm)	69.72	78.41	73.59	1.77	0.16
Height (mm)	45.03	54.28	49.93	1.67	0.35
Fruit index	0.65	0.69	0.68	0.05	0.00

Min = minimum; Max = maximum; S.D. = standard deviation; S.E. = standard error

Table 2S Results of model performance by PLS regression with interactance measurement mode and different spectral pretreatments

| | Pretreatment | F | Calibration model | | | Prediction model | | | | |
			R	RMSEC V	SEC	R	RMSE P	SEP	Bias	RPD
SSC	Raw	7	0.80	0.79	0.62	0.68	0.83	0.77	0.35	1.30
(%)	1-Der	6	0.74	0.83	0.71	0.82	0.59	0.60	-0.04	1.65
	2-Der	4	0.70	0.84	0.75	0.82	0.59	0.59	-0.12	1.68
	MSC	10	0.87	0.75	0.52	0.70	0.74	0.73	-0.19	1.37
	EMSC	9	0.86	0.78	0.54	0.82	0.58	0.58	-0.13	1.72
	OSC	6	0.89	0.64	0.47	0.58	0.89	0.90	-0.05	1.10
	SNV	10	0.87	0.75	0.52	0.70	0.74	0.73	-0.19	1.37
	EMSC+1-Der	1	0.59	0.86	0.85	0.65	0.78	0.77	-0.20	1.29
	EMSC+2-Der	1	0.58	0.86	0.85	0.58	0.82	0.81	-0.20	1.23
	EMSC+OSC	**6**	**0.86**	**0.71**	**0.54**	**0.82**	**0.58**	**0.57**	**-0.13**	**1.73**
	OSC+1-Der	14	0.92	0.60	0.42	0.55	0.89	0.91	0.02	1.09
	OSC+2-Der	2	0.77	0.73	0.66	0.78	0.66	0.62	0.25	1.60
ASC	Raw	10	0.90	8.87	6.45	0.92	5.54	5.29	0.19	2.54
(mg kg^{-1}FW)	1-Der	13	0.91	8.61	6.06	0.85	7.32	7.35	0.12	1.83
	2-Der	12	0.89	9.17	6.49	0.88	6.49	6.38	0.17	2.11
	MSC	9	0.89	8.95	6.55	0.91	6.16	5.81	0.23	2.32
	EMSC	8	0.89	8.82	6.61	0.91	5.87	5.53	0.22	2.43
	OSC	**5**	**0.89**	**8.39**	**6.52**	**0.92**	**5.56**	**5.31**	**0.19**	**2.54**
	SNV	9	0.89	8.98	6.55	0.91	6.17	5.81	0.23	2.32
	EMSC+1-Der	13	0.90	8.73	6.36	0.91	5.60	5.66	0.06	2.38
	EMSC+2-Der	11	0.90	8.60	6.40	0.91	5.55	5.54	0.11	2.43
	EMSC+OSC	3	0.88	8.30	6.84	0.91	5.91	5.75	0.17	2.34
	OSC+1-Der	7	0.89	8.42	6.56	0.83	7.45	7.58	0.00	1.78
	OSC+2-Der	7	0.90	8.36	6.45	0.84	7.18	7.27	0.07	1.85
Firmness	Raw	10	0.88	5.52	3.88	0.90	3.97	3.97	0.71	2.26
(N)	1-Der	11	0.84	5.66	4.38	0.81	5.24	5.31	0.46	1.69
	2-Der	10	0.84	5.65	4.33	0.88	4.41	4.45	0.55	2.02

	F	R	RMSECV	SEC	R	RMSEP	SEP		RPD
MSC	10	0.88	5.64	3.77	0.85	4.68	4.75	0.21	1.89
EMSC	12	0.91	5.37	3.32	0.82	5.03	5.11	-0.18	1.76
OSC	**4**	**0.87**	**4.90**	**4.00**	**0.89**	**4.21**	**4.20**	**0.86**	**2.14**
SNV	10	0.88	5.66	3.77	0.85	4.67	4.75	0.20	1.89
EMSC+1-Der	14	0.89	5.53	3.65	0.86	4.53	4.61	0.16	1.95
EMSC+2-Der	14	0.90	5.22	3.52	0.81	5.23	5.31	0.29	1.69
EMSC+OSC	7	0.90	4.84	3.43	0.83	4.97	5.05	-0.10	1.78
OSC+1-Der	7	0.85	5.01	4.20	0.82	5.09	5.14	0.57	1.75
OSC+2-Der	5	0.84	4.81	4.30	0.85	4.75	4.81	0.49	1.87

Raw: raw NIR spectra; 1-Der: Savitzky-Golay first derivatives; 2-Der: Savitzky-Golay second derivatives; MSC: Multiplicative scatter correction; EMSC: Extended multiplicative scatter correction; OSC: Orthogonal signal correction; SNV: Standard normal variate; F: Number of factor; R: Correlation of coefficient; RMSECV(P): Root mean square errors of cross validation (or prediction); SEC(P): Standard error of the calibration (or prediction); RPD: Residual predictive deviation (S.D. of the prediction/ SEP). SSC

Table 3S Results of model performance by PLS regression with reflectance measurement mode and different spectral pretreatments

| | Pretreatment | F | Calibration | | | Prediction | | | | |
			R	RMSECV	SEC	R	RMSEP	SEP	Bias	RPD
SSC	Raw	7	0.77	0.86	0.66	0.73	0.70	0.71	-0.08	1.41
(%)	1-Der	9	0.79	0.78	0.64	0.78	0.74	0.75	0.02	1.32
	2-Der	9	0.78	0.84	0.66	0.76	0.78	0.80	-0.04	1.25
	MSC	6	0.76	0.86	0.67	0.24	1.18	1.13	-0.40	0.88
	EMSC	3	0.70	0.84	0.75	0.25	1.04	1.01	-0.31	0.98
	OSC	2	0.76	0.76	0.68	0.64	0.78	0.77	-0.18	1.29
	SNV	6	0.76	0.86	0.67	0.26	1.16	1.11	-0.39	0.89
	EMSC+1-Der	8	0.80	0.79	0.62	0.79	0.70	0.71	-0.05	1.40
	EMSC+2-Der	8	0.79	0.82	0.64	0.79	0.65	0.62	-0.21	1.59
	EMSC+OSC	9	0.87	0.73	0.51	0.72	1.44	1.45	0.20	0.68
	OSC+1-Der	6	0.80	0.74	0.63	0.81	0.65	0.66	-0.05	1.50
	OSC+2-Der	**4**	**0.79**	**0.74**	**0.64**	**0.81**	**0.59**	**0.58**	**-0.13**	**1.70**
ASC	Raw	10	0.85	10.44	7.66	0.72	9.46	9.39	0.21	1.43
(mg kg^{-1}FW)	1-Der	13	0.88	9.70	6.79	0.82	7.58	7.71	0.01	1.75
	2-Der	11	0.87	9.52	7.22	0.83	7.53	7.65	0.04	1.76
	MSC	8	0.85	10.05	7.69	0.75	8.99	8.97	0.17	1.50
	EMSC	8	0.85	10.33	7.67	0.69	9.87	9.80	0.21	1.37
	OSC	3	0.85	9.35	7.70	0.73	9.26	9.21	0.19	1.46
	SNV	8	0.85	10.05	7.67	0.74	9.01	9.00	0.17	1.50
	EMSC+1-Der	14	0.90	9.03	6.46	0.81	7.92	8.05	0.01	1.67
	EMSC+2-Der	**11**	**0.87**	**9.25**	**7.06**	**0.84**	**7.20**	**7.32**	**0.02**	**1.84**
	EMSC+OSC	4	0.85	9.48	7.59	0.68	9.96	9.93	0.20	1.36
	OSC+1-Der	12	0.94	7.61	5.02	0.82	7.76	7.89	-0.01	1.71
	OSC+2-Der	10	0.92	8.06	5.56	0.82	7.53	7.66	-0.01	1.76
Firmness	Raw	7	0.79	6.04	4.90	0.77	5.80	5.76	1.28	1.56
(N)	1-Der	7	0.75	6.36	5.32	0.51	7.97	7.90	1.76	1.14

43

2-Der	8	0.79	6.31	4.90	0.57	7.51	7.50	1.42	1.20
MSC	7	0.81	6.09	4.68	0.75	5.94	5.97	0.86	1.50
EMSC	7	0.82	5.89	4.58	0.75	6.00	6.01	1.08	1.49
OSC	2	0.81	5.20	4.65	0.73	6.13	6.15	1.02	1.46
SNV	7	0.81	6.10	4.69	0.75	5.91	5.95	0.86	1.51
EMSC+1-Der	6	0.74	6.22	5.35	0.50	8.05	7.96	1.87	1.13
EMSC+2-Der	7	0.77	6.24	5.10	0.56	7.69	7.59	1.87	1.18
EMSC+OSC	**3**	**0.83**	**5.24**	**4.47**	**0.75**	**5.94**	**5.94**	**1.08**	**1.51**
OSC+1-Der	2	0.79	5.34	4.95	0.63	7.06	7.03	1.42	1.28
OSC+2-Der	3	0.80	5.39	4.81	0.61	7.26	7.20	1.60	1.25

Raw: raw NIR spectra; 1-Der: Savitzky-Golay first derivatives; 2-Der: Savitzky-Golay second derivatives; MSC: Multiplicative scatter correction; EMSC: Extended multiplicative scatter correction; OSC: Orthogonal signal correction; SNV: Standard normal variate; F: Number of factor; R: Correlation of coefficient; RMSECV(P): Root mean square errors of cross validation (or prediction); SEC(P): Standard error of the calibration (or prediction); RPD: Residual predictive deviation (S.D. of the prediction/ SEP).

Chapter 3

Summary

Comparison of reflectance and interactance modes of visible and near infrared spectroscopy for predicting persimmon fruit quality

This study aimed to investigate the feasibility of visible and short-wave near infrared spectroscopy (Vis/SWNIRS) for evaluating persimmon fruit quality. Two measurement techniques; interactance and reflectance were compared their performing abilities. Partial least square regression was used to develop prediction models for physical and chemical quality of intact persimmon fruit. The following conclusion can be drawn from all experimental results. Vis/SWNIRS was found to be feasible to predict soluble solids content, ascorbic acid, as well as physical quality like fruit firmness. The models from interactance measurement mode provided better prediction accuracy in all parameters. In addition, spectral preprocessing techniques can eliminate or reduce variability of spectral properties unrelated to the spectral property of interest.

Acknowledgements

Foremost, I would like to express my deep and sincere gratitude to my research supervisor at Niigata University, Professor Dr. Kazuhiro Nakano, for giving me the opportunity to do research and providing invaluable guidance throughout this research. His support, motivation and encouragement have deeply inspired me. I am very much appreciated the kindness and PhD scholar opportunities of double degree program he have provided.

My sincere gratitude also express to my supervisor at Chiang Mai University, Professor Dr. Danai Boonyakiat for his immense knowledge of postharvest technology and biology.

In addition, my sincere gratitude also express to Associate Professor Dr. Shintaroh Ohashi for his kindness, support and valuable guidance throughout my study in Niigata.

My sincere thanks also express to NASER laboratory members Dr. Phonkrit Maniwara, Dr. Somsak Kramchote and all other members for the stimulating discussion collaborating a good teamwork and insightful comments. I would not have been able to do this research work without their assistance.

I am gratefully acknowledged to the Double Degree Program (DDP) of Graduate School of Science and Technology, Niigata University for creating the wonderful program and giving me this opportunity to be part of this program.

Most importantly, I would like to express my gratitude to my parents, Mr. Ming Sae-Wui, Mrs. Meifong Sae-Yang, for raised me with all the love and kindness and being a constant source of strength and inspiration in my life.

References

Barrett DM, John CB, Rob S (2010) Color, flavor, texture, and nutritional quality of fresh-cut fruits and vegetables: Desirable levels, instrumental and sensory measurement and the effects of processing Crit Rev Food Sci Nutr 50:369-389. https://doi.org/10.1080/10408391003626322

Beebe KR, Pell RJ, Seasholtz MB (1998) Chemometrics: A Practical Guide, John Wiley and Sons, Chichester. UK, pp 348

Beever DJ, Hopkirk G (1990) Fruit development and fruit physiology. In IJ Warrington, GC Weston, eds, Kiwifruit: Science and Management. Ray Richards, New Zealand, pp. 97-126.

Blanco, M. and I. Villarroya. 2002. NIR spectroscopy: a rapid-response analytical tool. Trends in Analytical Chemistry 21: 240-250.

Brereton, R.G. 2009. Chemometrics for pattern recognition. John Wiley and Sons Ltd., Bristol, UK. Applied Spectroscopy 54: 1055-1068.

Brossard, J. and G. Mackinney. 1963. Carotenoids of *Diospyros kaki* (Japanese Persimmons). Journal of Agricultural and Food Chemistry 11(6): 501-503.

Brown, C.D., L. Vega-Montoto and P.D. Wentzell. 2000. Derivative preprocessing and optimal corrections for baseline drift in multivariate calibration.

Candir EE, Ozdemir AE, Kaplankiran, M, Toplu C (2009) Physico-chemical changes during growth of persimmon fruits in the east Mediterranean climate region. Sci Hortic 121:42-48. https://doi.org/10.1016/ j.scienta.2009.01.009

Celik, A. and S. Ercisli. 2008. Persimmon cv. Hachiya (*Diospyros kaki* T.) fruit: some physical, chemical and nutritional properties. International Journal of Food Science and Nutrition 59(7-8): 599-606.

Chang CW, Laird DA, Mausbach MJ, Hurburgh JCR (2001) Near-infrared reflectance spectroscopy principle components regression analysis of soil properties. Soil Sci Soc Am J 65:480-490. https://doi.org/10.2136/sssaj2001.652489x

Chen, X.N., J.F. Fan, X. Yue, X.R. Wu and L.T. Li. 2008. Radical scavenging activity and phenolic compounds in persimmon (*Diospyros kaki* L. cv. Mopan). Journal of Food Science 73: 24-28.

Clark, C.J., V.A. McGlone and R.B. Jordan. 2003. Detection of brownheart in 'Braeburn' apple by transmission NIR spectroscopy. Postharvest Biology and Technology 28: 87-96.

Cortés V, Alejandro R, José B, Beatriz R, Cristina B, Sergio C, Alejandra S, Pau T, Nuria A (2017) Prediction of the level of astringency in persimmon using visible and near-infrared spectroscopy. J Food Eng 204: 27-37. https://doi.org/10.1016/j.jfoodeng.2017.02.017

Cozzolino D, Cynkar W, Shah N, Smith P (2011) Feasibility study on the use of attenuated total reflectance mid-infrared for analysis of compositional parameter in wine. Food Res Int 44: 181-186. https://doi.org/10.1016/j.foodres.2010.10.043

Croce R, Malegori C, Oliveri P, Medici I, Cavaglioni A, Rossi C (2020) Prediction of quality parameters in straw wine by means of FT-IR spectroscopy combined with multivariate data processing. Food Chem 305: 125512. https://doi.org/10.1016/j.foodchem.2019.125512

Del Bubba M, Giordani E, Cincinelli A, Checchini L, Galvan, P (2009) Nutraceutical properties and sugar contents in astringent persimmons during on-tree growth and ripening and in response to different postharvest treatments. J Food Compos Anal 22: 668-677. https://doi.org/10.1016/ j.jfca 2009.02.015

Daood, H. G., P. Biacs, B. Czinkotai and A. Hoschke. 1992. Chromatographic investigation of carotenoids, sugars and organic-acids from *Diospyros-Kaki* fruit. Food Chemistry 45(2): 151-155

Ebert G, Gross J (1985) Carotenoid changes in the peel of ripening persimmon (Diospyros Kaki) cv Triumph. Phytochemistry 24: 29-32. https://doi.org/10.1016/S0031-9422(00)80801-8

Fahmy K, Kohei N (2016) Effective transport and storage condition for preserving the quality of 'Jiro' persimmon in export market. Agric Agric Sci Procedia 9: 279-290. https://doi.org/10. 1016/j.aaspro2016.02.115

Frizon CNT, Oliveira GA, Perussello CA, Peralta-Zamora PG, Camlofski AMO, Rossa UB, Hoffmann-Ribani R (2015) Determination of total phenolic compounds in yerbamaye (llex paraguariensis) combining near infrared spectroscopy (NIR) and multivariate analysis. LWT Food Sci Technol 60: 795-801. https://doi.org/10.1016/ j.jwt.2014.10.030

Geisser, S. 1964. Posterior odds for multivariate normal distributions. Journal of the Royal Statistical Society Series B (Statistical Methodology) 26: 69-76.

George, A.P. and S. Redpath. 2008. Health and medicinal benefits of persimmon fruit: a review. Advances in Horticultural Science 22: 244-249.

Giordani E, Doumett S, Nin S, Del Bubba M (2011) Selected primary and secondary metabolites in fresh persimmon (Diospyros kaki Thumb.): a review of analytical methods and current knowledge of fruit composition and health benefits. Food Res Int 44: 1752-1757. https://doi.org/10.1016/j.foodres.2011.01.036

Gunasekaran, S. and J. Irudayaraj. 2001. Optical Methods: Visible , NIR, and FTIR Spectroscopy. pp. 1-37. *In*: S. Gunasekaran (ed.). Nondestructive Food Evaluation Techniques to Analyze Properties and Quality. Marcel Dekker, Inc., New York.

Hou, S.R., Y.C. Feng and C.Q. Hu. 2008. Development of a near infrared method for rapid determination water content in ceftriaxone sodium for injection. Chinese Journal of Pharmaceutical Analysis 28: 936.

Huang Y, Lu R, Chen KJ (2018) Prediction of firmness parameters of tomatoes by portable visible and near-infrared spectroscopy. J Food Eng 222: 185-198. https://doi.org/10. 1016.j .jfoodeng.2007.11.030

Itoo, S. 1971. The persimmon. *In* A.C. Hulme (Ed.), The biochemistry of Fruits and their Products. Volume 2. pp. 281-301. London: Academic Press Inc. (London) Ltd.

Kawano, S. 1995. Progress in Application of NIR and FT-NIR in Food Characterization. pp. 185-199. *In*: A.G. Gaonkar (ed.). Characterization of Food: Emerging Methods. Elsevier Science B.V., Amsterdam.

Kawano, S. 2002. Sampling and Sample Presentation. pp. 115-124. *In*: H.W. Siesler, Y. Ozaki, S. Kawata and H.M. Seise (eds.). Near Infrared Spectroscopy: Principles, Instruments and Applications. Wiley-VCH, Weinheim.

Kays, S.E., F.E. Barton and W.R. Windham. 2000. Predicting protein content by near-infrared reflectance spectroscopy in diverse cereal food products. Journal of Near Infrared Spectroscopy 8: 33-43.

Krongchai, C., S. Funsueb, J. Jakmanee, S. Kittiwachana. 2016. Application of multiple self-organizing maps for classification of soil samples in Thailand according to their geographic origins. Journal of Chemometrics 31: 1-10.

Lammertyn J, Nicola B, Ooms K, De Smedt V, De Baerdemaeker J (1998) Non-destructive measurement of acidity, soluble solids, and firmness of 'Jonagold' apples using NIR spectroscopy. Trans ASAE 41: 1089-1094

Lammertyn, J., A. Peirs, J. Baerdemaeker and B. Nicolaï. 2000. Light penetration properties of NIR radiation in fruit with respect to non-destructive quality assessment. Postharvest Biology and Technology 18: 121-132.

Leardi, R. 2003. Chemometrics in data analysis. *In*: M. Lees (Ed.), Food Authenticity and Traceability (pp. 299-320), Cambridge, England: Woodhead Publishing Limited.

Liu H, Xiang B, Ou L (2006) Structure analysis of ascorbic acid using near-infrared spectroscopy and generalized two-dimensional correlation spectroscopy. J Mol Struct 794: 12-17. https://doi.org/10.1016/j/molstruc.2006.01.028

Lopez A, Arazuri S, Garcia I, Mangado J, Jaren C (2013) A review of the application of near-infrared spectroscopy for the analysis of potatoes. J Agri Food Chem 61: 5413-5424. https://doi.org/10.1021/jf401292j

Martelo-Vidal, M.J. and M. Vázquez. 2016. Advances in ultraviolet and visible light spectroscopy for food authenticity testing A2-Downey, Gerard. *In*: Advances in Food Authenticity Testing. Woodhead Publishing. pp. 35-70.

Malegori C, Marques EJN, de Freitas ST, Pimentel MF, Pasquini C, Casiraghi E (2017) Comparing the analytical performances of Micro-NIR and FT-NIR spectrometers in the evaluation of acerola fruit quality, using PLS and SVM regression algorithms. Talanta 165: 112-116. https://doi.org/10.1016/j.talanta.2016.12.035

Maniwara P, Nakano K, Boonyakiat D, Ohashi S, Hiroi M, Tohyama T (2014) The use of visible and near infrared spectroscopy for evaluating passion fruit postharvest quality. J Food Eng 143: 33-43. https://doi.org/10.1016/j.jfoodeng.2014.06.028

Matsuo T, Ito S, Ben-Arie R (1991) A model experiment for elucidating the mechanism of astringency removal in persimmon fruit using respiration inhibitors. J Jpn Soc Hortic Sci 60: 437-442. https://doi.org/ 10.2503/jjshs.60.437

McGlone, V.A., H. Abe and S. Kawano. 1997. Kiwifruit firmness by near infrared light scattering. Journal of Near Infrared Spectroscopy 5: 83-89.

McGlone, V.A., R.B. Jordan and P.J. Martinsen. 2002. Vis/NIR estimation at harvest of pre- and post-storage quality indices for 'Royal Gala' apple. Postharvest Biology and Technology 25: 135-144.

Mehinagic, E., G. Royer, R. Symoneaux, D. Bertrand and F. Jourjon. 2004. Prediction of the sensory quality of apples by physical measurements. Postharvest Biology and Technology 34: 257-269.

Munera S, Besada C, Aleixos N, Talens P, Salvador A, Sun DW, Cubero S, Blasco J (2017) Non-destructive assessment of the internal quality of intact persimmon fruit using colour and VIS/NIR hyperspectral imaging. LWT Food Sci Technol 77: 241-248. https://doi.org/10.1016/j.jwt.2016.11.063

Mowat, A.D. and P.R. Poole. 1997. Non-destructive discrimination of persimmon fruit quality using visible-near infrared reflectance spectrophotometry. Acta Horticulturae 436: 159-163.

Naes, T., T. Isaksson, T. Fearn and T. Davies, 2004. A User-friendly Guide to Multivariate Calibration and Classification. NIR Publications, Chichester. 344 p.

Nicolaï BM, Beullens K, Bobelyn E, Peirs A, Saeys W, Theron KI, Lammertyn J (2007) Non-destructive measurement of fruit and vegetable quality by means of NIR spectroscopy: a review. Postharvest Biol Technol 46: 99-118. https://doi.org/10.1016/j.postharvbio.2007.06.024

Nordey T, Jacques J, Fabrice D, Marc C, Mathieu L (2017) Robust NIRS models for non-destructive prediction of mango internal quality. Sci Hort 216: 51-57. https://doi.org/10.1016/j.scienta. 2016.12.023

Norris, K.H. 1964. Reports on design and development of a new moisture meter. Journal of Agricultural Engineering 45(7): 370-372.

Noypital S, Terdwongworakul A, Krisanapook K, Kasemsumran S (2015) Evaluation of astringency and tannin content in 'Xichu' persimmon using near infrared spectroscopy. Int J Food Prop 18: 1014-1028. https://doi.org/10.1018/10942912 .2014.884577

Osborne, B.G., T. Fearn and P.H. Hindle. 1993. Practical NIR Spectroscopy with Applications in Food and Beverage Analysis. Longman Scientific and Technical, Harlow.

Palou A, Jordi C, Marcelo B, Rafael L, Juana F, César MB, Josep MG, Manel A (2014) Characterization of the composition of paraffin waxes on industrial applications. Energy Fuels 28: 956-963. https://doi.org/10.1021/ef4021813

Park, Y.S., Leontowicz, H., Leontowicz, M., Namiesnik, J., Jesion, I. and Gorinstein, S. 2008. Nutraceutical value of persimmon (*Diospyros kaki* Thunb) and its influence

on some indices of atherosclerosis in an experiment on rats fed cholesterol-containing diet. Advances in Horticultural Science 22: 250-254.

Pedro, A.M.K. and M.M.C. Ferreira. 2007. Simultaneously calibration solids, sugars and acidity of tomato products using PLS2 and NIR spectroscopy. Analytica Chimica Acta 595: 221-227.

Piretti, M.V. 1991. Polyphenols constituents of the *Diospyros kaki* fruit: A review. Fitoterapia 62: 3-13.

Rinnan Å, F. Van Den Berg, S.B. Engelsen. 2009. Review of the most common pre-processing techniques for near-infrared spectra. Trends in Analytical Chemistry 28(10): 1201-1222

Roy, S.K., D.S. Khurdiya and D.P. Waskar. 1995. Phalsa (In): Handbook of Fruit Science and Technology Production, Composition, Storage and Processing (Eds; D.K. Salunkhe and S.S. Kadam), Marcel Dekker, Inc., New York: 553-555.

Santos-Buelga, C. and A. Scalbert. 2000. Proanthocyanidins and tannin-like compounds–nature, occurrence, dietary intake and effects on nutrition and health. Journal of the Science of Food and Agriculture 80: 1094-1117.

Savitzky, A. and M.J.E. Golay. 1964. Smoothing and differentiation of data by simplified least squares procedures. Analytical Chemistry 36: 1627-1639.

Schaare PN, Frazer DG (2000) Comparison of reflectance, interactance and transmission modes of visible-near infrared spectroscopy for measuring internal properties of kiwifruit (Actinidia chinenensis). Postharvest Biol Technol 20: 175-184. https://doi.org/10.1016/S0925-5214(00)00130-7

Shah N, Cynkar W, Smith P, Cozzolino D (2010) Use of attenuated total reflectance mid-infrared for rapid and real-time analysis of compositional parameters in commercial white grape juice. J AgricFood Chem 58: 3279-3283. https://doi.org/10.1021/jf100420z

Slaughter, D.C., J.F. Thompson and E.S. Tan. 2003. Nondestructive determination of total soluble solids in fresh prune using near infrared spectroscopy. Postharvest Biology and Technology 28: 437-444.

Takekawa K. and K. Masumoto. 2012. Modification of cell wall polysaccharide during ripening of Chinese bayberry fruit. Scientia Horticulturae 160: 155-162.

Teerachaichayut, S., K.Y. Kil, A. Terdwongworakul, W. Thanapase and Y. Nakanishi. 2007. Non-destructive prediction of translucent flesh disorder in intact

mangosteen by short wavelength near infrared spectroscopy. Postharvest Biology and Technology 43: 202-206.

Terdwongworakul, A., N. Nakawajana., S. Teerachaichayut and A. Janhiran. 2012. Determination of translucent content in mangosteen by means of near infrared transmittance. Journal of Food Engineering 109: 114-119.

Uchida, S., Ohta, H., Niwa, M., Mori, A., Nonaka, G. and Nishioka, I. 1990. Prolongation of life span of stroke-prone spontaneously hypertensive rats (SHESP) ingesting persimmon tannin. Chemical and Pharmaceutical Bulletin 38: 1049-1052.

USDA 2016. United States Department of Agriculture, Agriculture Research Service, Food Composition Database. Retrieved from https://www.nal.usda.gov

USDA. 2020. United States Department of Agriculture, Agriculture Research Service, Food Composition Database. Retrieved from https://www.nal.usda.gov

Van Buren, J.P. 1979. Chemistry of texture in fruits and vegetables. Journal of Texture Studies 10(1): 1-23.

Veberic R, Juhar J, Mikulic-Petkovsek M, Stampar F, Schmitzer V (2010) Comparative study of primary and secondary metabolites in 11 cultivars of persimmon fruit (Diospyros kaki L.). Food Chem 119: 477-483. https://doi.org/10.1016/j.foodchem.2009.06.044

Vitale R, Bevilacqua M, Bucci R, Magrì AD, Magrì AL, Marini F (2013) A rapid and non-invasive method for authenticating the origin of pistachio samples by NIR spectroscopy and chemometrics. Chemom Intell Lab Syst 121: 90-99. https://doi/10.1016/j.chemolab.2012.11.019

Wang J, Jun W, Zhou C, Donghai H (2017) Development of multi-cultivar models for predicting the soluble solid content and firmness of European pear (Pyrus communis L.) using portable vis-NIR spectroscopy. Postharvest Biol Technol 129: 143-151. https://doi.org/10.1016/j.postharvbio. 2017.03.012

Williams P (2007) Near-infrared technology getting the best out of light, ed 5. A short course in the practical implementation of near-infrared spectroscopy for the user. PDK Grain, Nanaimo, Canada

Winton A.L. and K.B. Winton. 1935. The Structure and Composition of Foods. Vol. 2. NY: John Wiley & Sons, Inc. New York

Wold S, Henrik A, Fredrik L, Jerker Ö (1998) Orthogonal signal correction of near-infrared spectra. Chemom Intell Lab Syst 44: 175-185. https://doi.org/10.1016/S0169-7439(98)00109-9

Wold, S., M. Sjöstrom and L. Eriksson. 2001. PLS-regression: a basic tool of chemometrics. Chemometrics and Intelligent Laboratory Systems 58: 109-130.

Xie, L., X. Ye, D. Liu and Y. Ying. 2011. Prediction of titratable acidity, malic acid, and citric acid in bayberry fruit by near-infrared spectroscopy. Food Research International 44: 2198-2204.

Xing J.S. and X.B. Zhang. 2010. Development of a near-infrared method for rapid determination of ampicillin capsules. Chinese Journal of Pharmaceutical Analysis 30: 2408-2411.

Yee NG, George GC (2003) Orthogonal signal correction of potato crisp near infrared spectra. J Chin Inst Chem Eng 34: 563-574

Yonemori K, Sugiura A,Yamada M (2000) Persimmon genetics and breeding. Plant Breeding Rev 19:191-225

Yonemori, K., A. Ikegani, S. Kanzaki and A. Sugiura. 2003. Unique features of tannin cells in fruit of pollination constant non-astringent persimmons. Acta Horticulturae 601(1): 31-35.

Yuan B, Xu HL, Leng SP (2006) Content and chemicals composition of carotenoids in persimmon fruit. Chin Agric Sci Bull 22: 277-280

Zheng QL, Nakatsuka A, Itamura H (2006) Involvement of negative feedback regulation in wound-induced ethylene synthesis in 'Saijo' persimmon. J Agric Food Chem 54: 5875-9. https://doi.org/10 .1021/jf060048h

Zhou, C.H., D.Q. Zhao, Y.L. Sheng, J. Tao and Y. Yang. 2011. Carotenoids in fruits of different persimmon cultivars. Molecules 16(1): 624-636.